nature portfolio

https://doi.org/10.1038/s41551-022-00909-y

## Supplementary information

# Mapping and targeted viral activation of pancreatic nerves in mice reveal their roles in the regulation of glucose metabolism

In the format provided by the authors and unedited

**CONTENTS**

**Supplementary Methods**

**Surgical Procedures: Dual Pancreas and Liver injection**
Intrapancreatic injections were performed as described previously, $1*10^{11}$(Dose 1) viral genomes of AAV8-hSyn-mCherry were injected in WT mice. Three weeks later, 10 $\mu$l of Cholera Toxin B (CTβ) at concentration 8 $\mu$g/$\mu$L were injected in 1$\mu$L increments into all lobes of the liver. After 1 week, animals were sacrificed as described previously. CG were fixed, prepared for cryosection and stained for CTβ and mCherry as described above. The quantification of mCherry+ and CTβ+ neurons overlap was done using the JaCOP plugin by FIJI.

**Tissue Processing: Cryosections**
Heart, kidneys, brain and muscles were immersed in 30% sucrose (Sigma-Aldrich, 50389) in PBS overnight, then embedding in O.C.T Compound (Thermofisher Scientific; 23-730-572), frozen at -80C, and sectioned at 10 $\mu$m thickness. Tissues were stained overnight for mCherry (Abcam; ab205402) + synapsin1 (Cell Signaling; 5297S) at 1:1000 dilution. GFP (AVES, Tigard, OR; GFP-1020), at 1:1000 dilution) Subsequent secondary antibodies used were Alexa Fluor 546 anti-rabbit (Thermofisher Scientific; A10040), Alexa Fluor 647 anti-chicken (Jackson ImmunoResearch; 703-605-155) and Alexa Fluor 647 anti-chicken (Jackson ImmunoResearch; 703-605-155, Lot#138591). Tissues were stained for DAPI and coverslipped as stated previously. Samples were visualized using a fluorescent Zeiss Axio Observer Z.1 microscope.

***Ex vivo* Calcium Imaging**
AAV-hSyn-hM3D(Gq)-mCherry was administered to Snap25-2A-GCaMP6s-D via intraductal infusion (5*1011 (Dose 2)). Four weeks post-injection animals were anesthetized, as described above and CG dissected and placed in glass bottom 35 $\mu$m dish (Ibidi, # 81158) and incubated in HEPES-buffered solution (125 mM NaCl, 5.9 mMl KCl, 2.56 mM CaCl2, 1 mM MgCl2, 25 mM HEPES, 0.1% BSA [wt/vol.], 3mM D-glucose pH 7.4) at 37oC and 5% CO2, for 30 min. Imaging was performed using a Zeiss LSM 880 confocal microscope with a 10X (NA: 0.3). Briefly, Z-stacks of the whole CG was acquired at a temporal resolution of 10 s. CNO (20 $\mu$M) was administered after 20 s and KCl stimulation (50mM) at 10 min was performed to confirm neuronal responsiveness. Image analysis was performed using FIJI. Briefly regions of interests (ROI) were selected for background, mCherry+ neurons and mCherry– neurons, and mean intensity was calculated for every ROI in each image. Calcium responses were quantified as fluorescence intensity normalized to baseline fluorescence.

## Supplementary Figures

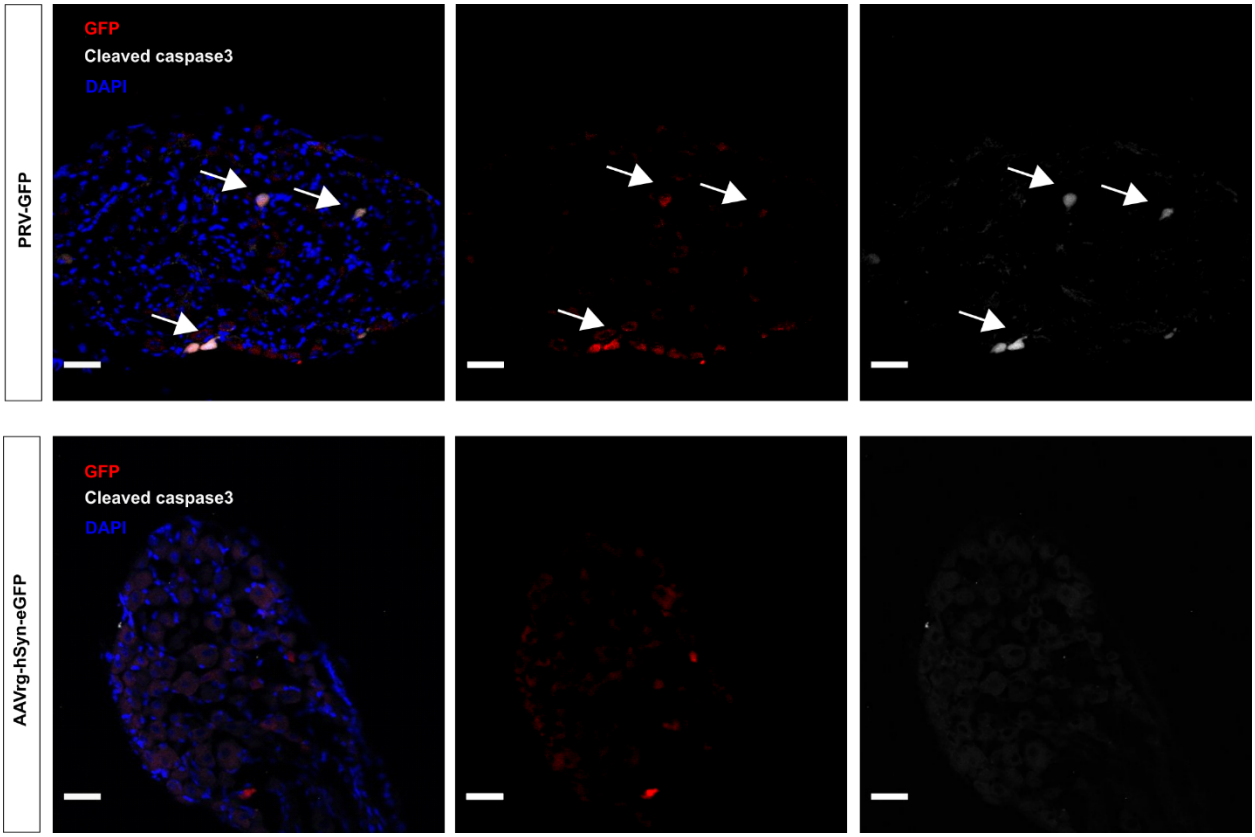


**Supplementary Fig. 1 | AAVs do not elicit apoptosis in transduced neurons**.
Representative immunofluorescence images of cleaved caspase-3 (white), GFP (red) and DAPI (blue) in NG sections, from mice 3 days after intrapancreatic injection of PRV-GFP ($2*10^6$ vg) and 4 weeks after intrapancreatic injection of rAAV2retro-hSyn-GFP ($1*10^{11}$ vg). One study, 2 samples per group. Scale bars: 50 $\mu$m.

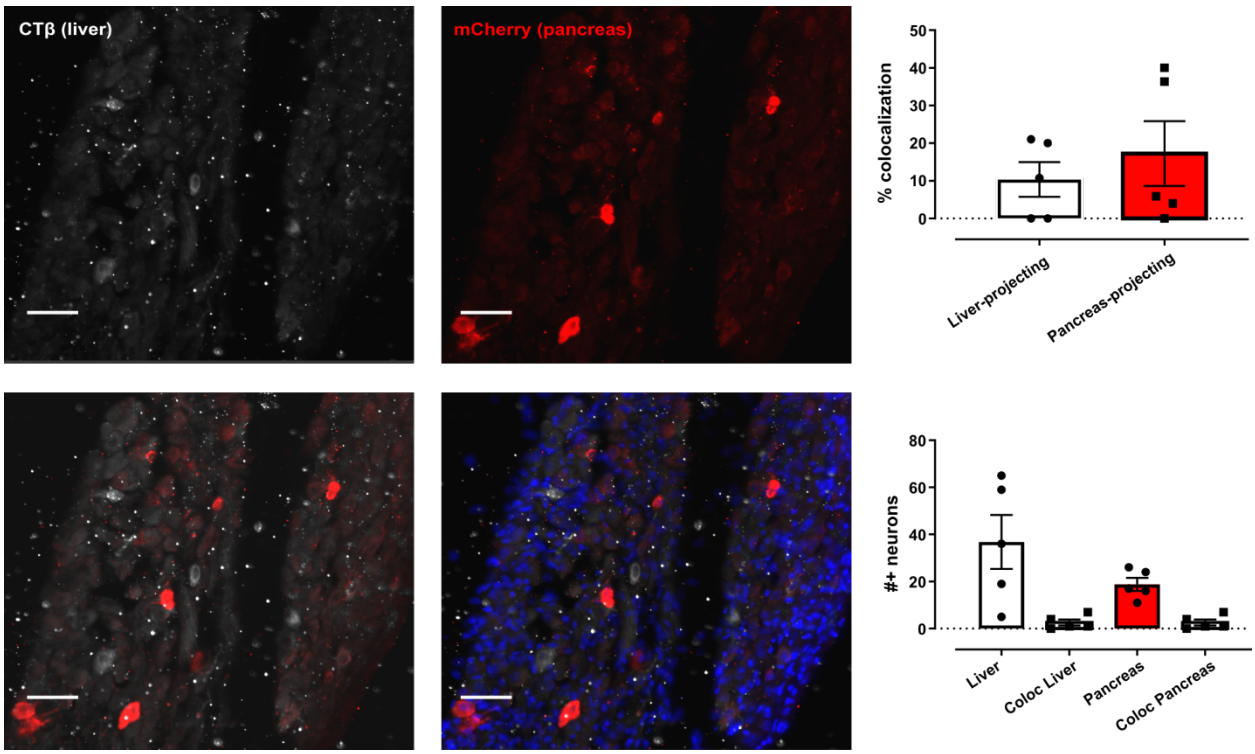


**Supplementary Fig. 2 l Assessment of colocalization of pancreas and liver-projecting neurons in the CG.** Representative immunofluorescence images of CG from mice that received AAV8-hSyn-mCherry via intrapancreatic injection (mCherry+ pancreas-projecting neurons in red) and CTβ via liver injection (CTβ+ liver-projecting neurons in white) N= 5 mice/group. Scale bars: 50 $\mu$m. Right upper panel, quantification of percentage of pancreas-projecting neurons that colocalize with liver-projecting neurons and percentage of liver-projecting neurons that colocalize with pancreas-projecting neurons. Bottom right panel, number of pancreas-projecting neurons, pancreas-projecting neurons that colocalize with liver-projecting neurons, liver-projecting neurons and liver-projecting neurons that colocalize with pancreas-projecting neurons. Data are shown as mean ± SEM.

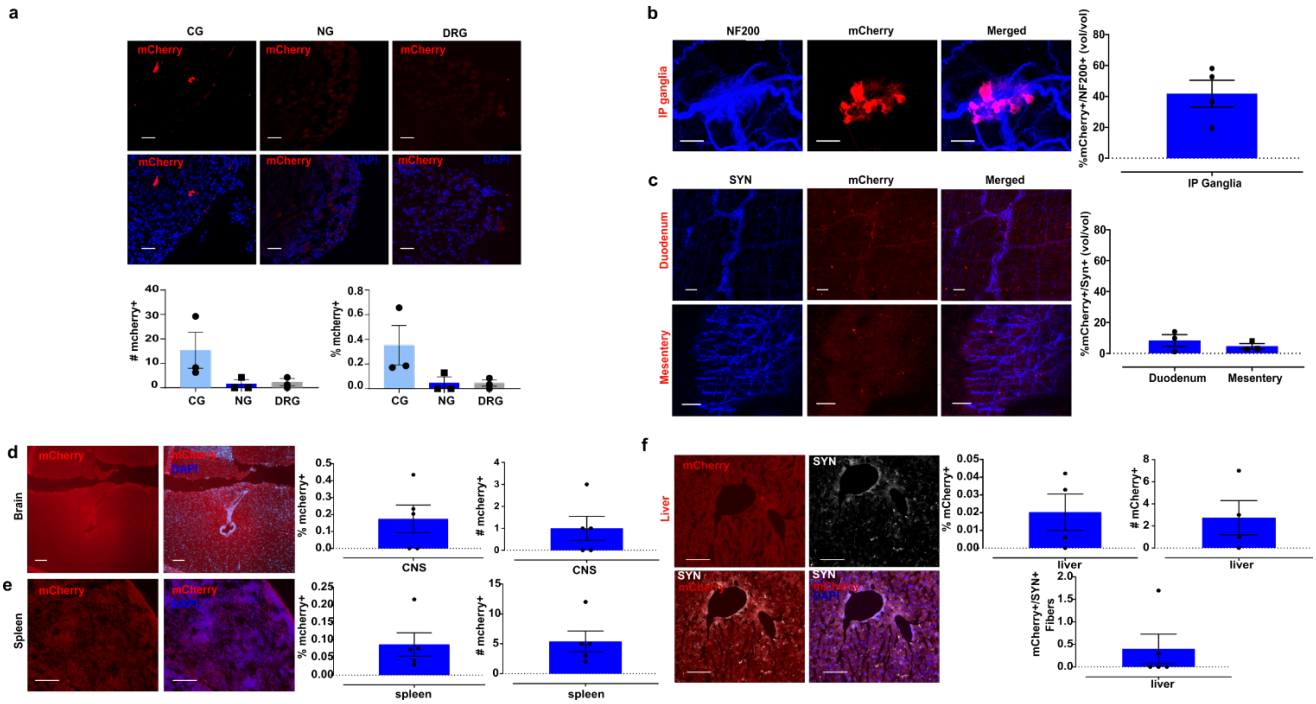


**Supplementary Fig. 3 l Assessment of AAV8-hSyn-DIO-hM3D(Gq)-mCherry expression in ChAT-IRES-CRE mice in ganglia, gut, liver, spleen and CNS. a)** Representative immunofluorescence images of CG, NG and DRG after intraductal infusion of AAV8-hSyn-DIO-hM3D(Gq)-mCherry ($5*10^{11}$ vg) in ChAT-IRES-cre mice showing mCherry (red) and DAPI (blue). Scale bars: 50 $\mu$m. Lower panels: quantification of total mCherry+ cells (left) and as a percentage of DAPI+ cells (right). N= 3 mice/group. **b)** Maximum projection confocal images of iDISCO+ cleared pancreas demonstrating expression of mCherry+ pancreas-innervating neurons (red) within IP ganglia stained for NF200 (blue) Scale bars: 50 $\mu$m. Right panel: Quantification of mCherry+ expression as percentage of NF200+ intrapancreatic ganglia volume. N= 4 mice**.** **c)** mCherry+ expression (red) in duodenal and mesenteric innervation stained for Synapsin (blue) Scale bars: 50 $\mu$m. Right panel: quantification of mCherry+ expression as percentage of total Synapsin+ volume. N = 3 mice. **d)** Representative images of mCherry (red) and DAPI (blue) in hindbrain, showing minimal viral expression of AAV8-hSyn-DIO-hM3D(Gq)-mCherry in ChAT-IRES-cre mice. Scale bars: 100 $\mu$m. Right panel: quantification of mCherry+ cells as a percentage of DAPI+ cells (left) and as total number (right). N = 5 mice. **e)** Representative images of mCherry (red) and DAPI (blue) in spleen, showing minimal viral expression of AAV8-hSyn-DIO-hM3D(Gq)-mCherry in ChAT-IRES-cre mice. Scale bars: 100 $\mu$m. Right panel: quantification of expression of the mCherry+ cells as a percentage of DAPI+ cells (left) and as total number (right). N = 5 mice. **f)** Representative images of mCherry (red), synapsin (white) and DAPI (blue) in liver, showing minimal viral expression in liver cells (N= 4 mice) and minimal overlap with synapsin+ fibers of AAV8-hSyn-DIO-hM3D(Gq)-mCherry in ChAT-IRES-cre mice (N= 5 mice). Scale bars: 100 $\mu$m. Right upper panel: quantification of expression of mCherry+ cells as a percentage of DAPI+ cells (left) and as total number (right). Lower right panel: quantification of overlap of mCherry+ and synapsin+ fibers.
Data are shown as mean ± SEM.

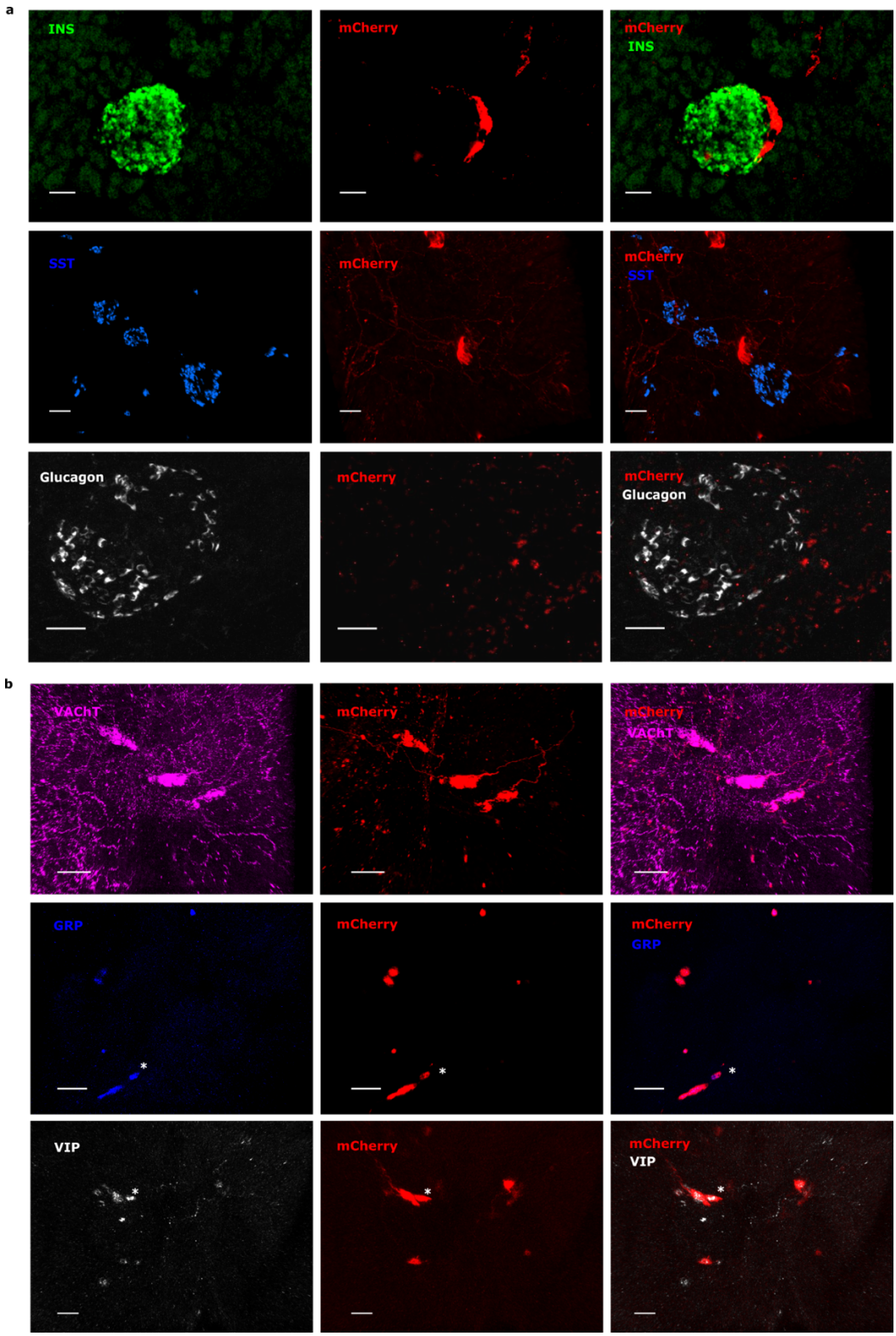


**Supplementary Fig. 4 | Assessment of AAV8-hSyn-DIO-hM3D(Gq)-mCherry expression in ChAT-IRES-CRE mice in pancreatic islets and with neural markers in intrapancreatic ganglia. a)** Representative confocal images of iDISCO+ cleared pancreas from ChAT-IRES-cre/AAV8-hSyn-DIO-hM3D(Gq)-mCherry mice stained for insulin (INS, green), somatostatin (SST, blue), glucagon (white) showing no overlap with viral expression (mCherry, red). One study, 2 samples per group. Scale bars: 50 $\mu$m. **b)** Representative confocal images of iDISCO+ cleared pancreas, stained for parasympathetic markers VAChT (magenta), Gastrin Release Peptide (GRP, blue) and Vasoactive Intestinal Peptide (VIP, white), showing co-expression with mCherry+ (red) neurons. Co-localization of neural markers with mCherry is indicated by asterisks. One study, 2 samples per group. Scale bars: 50 $\mu$m.

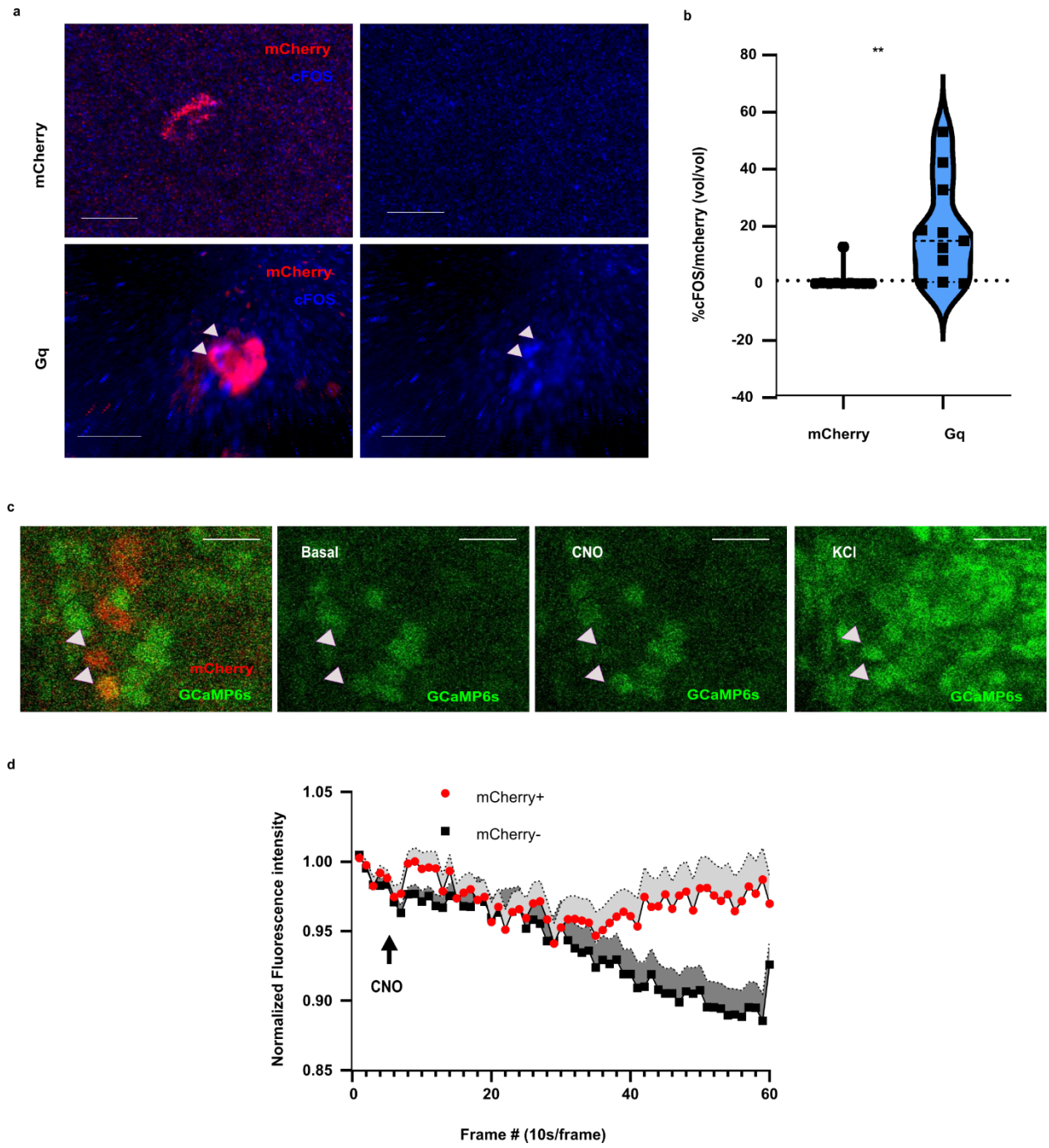


**Supplementary Fig. 5 l Activation of pancreas-projecting neurons expressing chemogenetic constructs by CNO. a)** Representative confocal images of mCherry+ (red) intrapancreatic ganglia and cFOS (blue) in pancreas of CNO-treated ChAT-IRES-cre/AAV8-hSyn-DIO-mCherry mice (upper panel) and CNO-treated ChAT-IRES-cre/AAV8-hSyn-DIO-hM3D(Gq)-mCherry mice (lower panel). Scale bar: 50 $\mu$m. **b)** Quantification of cFOS+ expression in mCherry+ intrapancreatic ganglia of CNO-treated ChAT-IRES-cre/AAV8-hSyn-DIO-hM3D(Gq)-mCherry (11 ganglia from 3 mice) and CNO-treated ChAT-IRES-cre/AAV8-hSyn-DIO-mCherry mice (control) (10 ganglia from 3 mice). cFOS volume expressed as percentage of mCherry+ volume of the ganglia. Two-tailed Mann-Whitney test, **p=0.005. **c)** Representative images of mCherry+ pancreas-projecting neurons in the CG from Snap25-2A-GCaMP6S mice, 4 weeks after intrapancreatic injection of AAV8-hSyn-hM3D(Gq)-mCherry, showing mCherry expression, basal fluorescence, response to CNO (20 $\mu$M) and KCl (50 mM). 3 independent replicates Scale bar Scale bar: 50 $\mu$m**. d)** Normalized Fluorescence Intensity ($F/F_0$) of mCherry+ neurons and mCherry- neurons in CG after CNO treatment (N=3 mice)

**Supplementary Tables**

**Supplementary Table 1 l** Quantification of total number of neurons per ganglia. Data are shown as mean ± SEM.

| Ganglia | # Neurons |
|---|---|
| CG | 1470.857 ± 556.654 (7) |
| L-NG | 13332 ± 394.475 (9) |
| R-NG | 994.8 ± 208.252 (8) |
| L-DRG10 | 1171.5 ± 187.044 (10) |
| L-DRG13 | 1269.286 ± 235.551 (10) |
| R-DRG10 | 1133.714 ± 231.999 (10) |
| R-DRG13 | 1365.143 ± 224.428 (9) |
| All NGs | 1000.529 ± 319.882(17) |
| All DRGs | 1042.769 ± 217.256 (39) |

**Supplementary Table 2 l** Statistical details for Figs. 1–7.

| Figure number and title | Statistical Details |
|---|---|
| **Fig. 1 l Pancreas is innervated by neurons in coeliac, nodose, dorsal root and intrapancreatic ganglia.** | One-way ANOVA was used for statistical analyses with multiple comparisons corrected by Tukey post-hoc test. **e**: left panel, p = 0.6335, F = 0.725; right panel, p = 0.841, F = 0.4445). p represents statistical significance and F represents the F-statistic.<br>Data are shown as mean ± SEM. |
| **Fig. 2 l AAV serotypes selectively target pancreatic autonomic efferent and afferent nerves.** | Panel **c** left: Kruskal-Wallis test between serotypes in CG, NG and DRG, p = 0.001, 0.002 and 0.003; $\chi^2_{(3)}$ = 15.57, 14.96 and 14.17 respectively. Multiple comparisons corrected by Dunn's multiple comparison test: CG: AAV9 vs AAV6 p=0.0033, AAV9 vs AAV6 p=0.024, AAV8 vs AAVrg p=0.031. NG: AAV9 vs AAV8 p=0.005, AAV8 vs AAVrg p=0.008. DRG: AAV9 vs AAV8 p=0.013, AAV8 vs AAVrg p=0.002.<br>Panel **c**, right: Kruskal-Wallis test between serotypes in CG, NG and DRG, p = 0.001, 0.004 and 0.001, $\chi^2_{(3)}$ = 17.04, 13.29 and 15.66 respectively. Multiple comparisons corrected by Dunn's multiple comparison test: CG:AAV8 vs AAV6 **p=0.006 AAV8 vs AAVrg *p=0.012. NG: AAV9 vs AAV8 *p=0.01, AAV8 vs AAVrg *p=0.013. DRG: AAV9 vs AAVrg *p=0.021, AAV8 vs AAVrg *p=0.049, AAV6 vs AAVrg **p=0.009.<br>Panel **d**: One-way ANOVA p = 0.468, F = 0.903 corrected using Tukey posthoc test.<br>Data are shown as mean ± SEM. |
| **Fig. 3 l Optimization of gene delivery** | Statistical analyses between IP and ID delivery used two-tailed Mann-Whitney U test in:<br>Panel **b**. For CG, L-NG, R-NG, L-DRG10, L-DRG13, R-DRG10, R-DRG13; P=0.057, 0.486, 0.487, 0.309, 0.885, 0.904, 0.334 respectively.<br>Kruskal-Wallis test with Dunn's multiple comparison test was used for dose response analyses.<br>Panel **d**: p = 0.057 $\chi^2_{(3)}$ = 10.86,<br>Panel **f**: p = 0.137, $\chi^2_{(3)}$ = 6.98, upper left, p = 0.117, $\chi^2_{(3)}$ = 7.39 upper right; p = 0.616, $\chi^2_{(3)}$ = 2.66 lower left, p = 0.628, $\chi^2_{(3)}$ = 2.60 lower right).<br>Data are shown as mean ± SEM. |

| | |
|---|---|
| **Fig.4 l Combined strategy for restricted gene expression in pancreatic innervation.** | Kruskal-Wallis test was used for statistical analyses:<br>**c**: left, n = 3 replicates/group, ***p<0.0001, $\chi^2_{(3)}$ = 248.5 using Dunn's multiple comparison test; right panel, n = 3 replicates/group ***p<0.0001, $\chi^2_{(3)}$ = 50.62 using Dunn's multiple comparison test).<br>Two-tailed Mann-Whitney test was used for statistical analysis of mCherry+ cells in liver<br>**g:** *p=0.029 (left), **h**: p=0.690 and **i:** p=0.184.<br>Two-tailed unpaired t-test was used for mCherry+ cells in CG, p=0.5739 (**g**, right).<br>Data are shown as mean ± SEM. Each *in vitro* study was performed 3 times with 3 technical replicates on each occasion. |
| **Fig. 5 l Pancreas parasympathetic activation improves glucose control.** | Two-way ANOVA with Sidak's multiple comparisons test for panel **b**: p=0.007, F=2.825. **p=0.003(15'), **p=0.003(30'), **p=0.003(45'), *p=0.013(60'), **p=0.008(90'), **p=0.004(120'), panel c: p=0.134, F=1.631<br>panel **d**: p<0.0001, F=15.09. *p=0.018(0'), ***p=0.0004(15'), ****<p=0.0001(30'), ****<p=0.0001 (45'), ***p=0.0005(60'), ***p=0.0004(90'), *p=0.0432(120')<br>panel **e**, left: p<0.0001, F=5.701. mCherry vs Gq: *p=0.0163(15'), **p=0.0072(30'), *p=0.0157(45'), *p=0.0168(90'), mCherry-Atropine vs Gq: *p=0.0175(15'), **p=0.0010(30'), **p=0.0027(45'), **p=0.0052(60'), *p=0.0208(90')<br>panel **f**: p=0.216, F=1.417 and panel **g**: p=0.006, F=5.60. *p=0.045(0'), *p=0.013(15').<br>Mixed-Effect analysis with Sidak's multiple comparisons for:<br>panel **h**: p=0.671, F=0.639. *p=0.028(15'). Panel **i:** p=0.419. Krustal-Wallis test for panel e, right; p=0.03, $\chi2(2)$ =13.64 with Dunn's multiple comparisons test. mCherry vs Gq **p=0.0026, mCherry-Atropine vs Gq *p=0.0253.<br>Two-tailed Mann-Whitney test for AUC for panel **b**, right: ***p<0.0001, panel **c**, right: p=0.0653.<br>Two-tailed unpaired t-test for panel **d**, right: ***p<0.0001.<br>Data are shown as mean ± SEM. |
| **Fig. 6 l Effects of ablation of parasympathetic pancreatic innervation.** | Two-tailed Mann-Whitney test was used for statistical analyses in panel **b**: *p=0.016 and panel **c**: left, p= 0.904, center, p=0.167, right, p= 0.142.<br>Two-way ANOVA was used for statistical analyses in panel **d:** p=0.753, F=0.568. panel **g**: p=0.917, F=0.330. panel h: p=0.241, F= 1.389. All analyses were corrected by Sidak's multiple comparisons test.<br>Two-tailed Paired t-test was used for statistical analysis in panel **e:** left p= 0.112, right *p= 0.032.<br>Mixed-Effect analysis was used for statistical analysis corrected by Sidak's multiple comparisons for panel **i**: p=0.917, F=0.166.<br>Data are shown as mean ± SEM. |
| **Fig. 7 l Pancreas sympathetic activation impairs glucose homeostasis** | Two-way ANOVA with Sidak's multiple comparison test was used for statistical analyses in panel **c**: p=0.023, F=2.418. panel d: p=0.040, F=2.18, *p=0.013 (30') and *p=0.030 (45'), panel **e**: , p=0.684, F=0.688. panel f: p=0.475, F=0.944.<br>Mixed-Effect analysis with Sidak's multiple comparison test was used for panel **g**: p=0.391, F=1.021 and **h**: p= 0.506, F= 0.713.<br>Two-tailed unpaired t-test was used in panel **c**, right: p=0.629. panel **d**, right: *p=0.020, panel **e**, right: p=0.263 and panel **f**, right: p = 0.1833<br>Data are shown as mean ± SEM. |

**Supplementary Table 3.** Statistical details for Extended Data Figs. 1–4.

| Figure number and title | Statistical Details |
|---|---|
| **Extended Data Fig. 1 l Distribution of CTβ+ pancreas–innervating neurons across ganglia** | Two-tailed Mann-Whitney test, n = 3 mice, 402 CTβ+ pancreas-innervating neurons for CG, 304 CTβ+ pancreas-innervating neurons for L-NG, 251 CTβ+ pancreas-innervating neurons for R-NG, 264 CTβ+ pancreas-innervating neurons for L-DRG, 141 CTβ+ pancreas-innervating neurons for R-DRG: L-NG vs. R-NG, ****p<0.0001, L-DRGs vs. R-DRGs, **p=0.001).<br>Data are shown as mean ± SEM. |
| **Extended Data Fig 2. l Off-target expression after intrapancreatic delivery of AAV** | Kruskal-Wallis test, corrected using Dunn's multiple comparison test. **b**: lower panel, p = 0.521, $\chi^2_{(3)}$ = 2.449, c: lower panel, p = 0.475, $\chi^2_{(3)}$ = 2.744, **d**: upper panel, p = 0.534, $\chi^2_{(3)}$ = 2.188, lower panel, p= 0.511, $\chi^2_{(3)}$ = 2.310, **e**: upper panel p = 0.002, $\chi^2_{(3)}$ = 14.45 *p=0.020 AAV9 vs AAVrg, *p=0.033 AAV8 vs AAVrg; lower panel p = 0.002, $\chi^2_{(3)}$ = 14.69, **f**: upper panel p = 0.034, $\chi^2_{(3)}$ = 8.67; *p=0.050 AAV8 vs AAV6, lower panel p = 0.085, $\chi^2_{(3)}$ = 6.67.<br>Data are shown as mean ± SEM. |
| **Extended Data Fig 3. l Neuronal specific promoters for gene delivery into pancreatic innervation.** | One-way ANOVA corrected by Tukey's multiple comparison test used for panel **c**, left panel: HEK293T cells, p < 0.0001, F = 108.1. JeT vs hSyn ****p<0.0001, JeT vs NSE ****p<0.0001, N2A cells, p < 0.0001, F = 50.90. JeT vs hSyn ****p<0.0001, JeT vs NSE ****p<0.0001, hSyn vs NSE **p=0.009. Panel **c**, right: HEK293T cells, p < 0.0001, F = 108.1. JeT vs hSyn ****p<0.0001, JeT vs NSE ****p<0.0001, N2A cells, p < 0.0001, F = 38.86. JeT vs hSyn ****p<0.0001, hSyn vs NSE **p=0.002. Panel **d**, right: HEK293T cells, p < 0.0001, F = 95.12. JeT vs hSyn ****p<0.0001, JeT vs NSE ****p<0.0001, N2A cells, p < 0.0001, F = 50.90. JeT vs hSyn ****p<0.0001, JeT vs NSE ****p<0.0001, hSyn vs NSE**p=0.002.<br>Krustal-Wallis corrected by Dunn's multiple comparison test used for panel **d**, left: HEK293T cells, p = 0.0037, $\chi^2_{(2)}$ = 11.19. JeTvs.hSyn **p=0.003, JeTvs.NSE *p=0.044, N2A cells, p = 0.021, $\chi^2_{(2)}$ = 7.776. JeTvs.hSyn *p=0.019<br>Two-tailed Mann-Whitney test was used for panels **e** and **f**.<br>Data are shown as mean ± SEM. |
| **Extended Data Fig 4. l CNO does not affect GTT in wild-type (WT) mice and female ChAT-IRES-cre/AAV8-Syn-DIO-hM3D(Gq)-mCherry.** | Two-way ANOVA corrected by Sidak's multiple comparisons tests **a**: p=0.811, F=0.530. **b**: p<0.001, F=4.552. (*p=0.022(15'), *p=0.010(30'), *p=0.0145(45'), *p=0.0132(90') **c**: p=0.130, F =1.667. **d**: p=0.351, F=1.137. **e**: p=0.155, F=1.464. **f**: p=0.674, F=0.698. **g**: p=0.025, F= 2.483. **h**: p=0.015, F=52.729. **i**: p=0.993, F=0.122. Mixed-Effect analysis with Sidak's multiple comparisons **m:** p=0.018, F=4.977. **n:** p=0.994, F=1.050. **o**: p=0.677, F=0.868. Two-tailed Mann-Whitney test (right **b**: **p=0.001, right **d**: p=0.104). Two-tailed Unpaired t-test (right **a**: p=0.573. **c**: p=0.913. **j**: p=0.407. **k**: p=0.114. **l**: p=0.375.<br>Data are shown as mean ± SEM |

**Captions for the Supplementary Videos**

**Supplementary Video 1** | Lightsheet microscopy images of mouse pancreatic samples cleared with iDISCO+ and immunostained for insulin (blue) and vesicular acetylcholine transporter (VAChT, white) demonstrating dense parasympathetic innervation and intrapancreatic ganglia. (https://drive.google.com/file/d/1l7DauzJ95DiU0xp6eLpHt-SHo_1fpa2J/view?usp=sharing)

**Supplementary Video 2** | Lightsheet microscopy images of mouse pancreatic samples cleared with iDISCO+ and stained for insulin (blue) and tyrosine hydroxylase (TH, white) demonstrating dense catecholaminergic innervation of the pancreas. (https://drive.google.com/file/d/1KDvqx6sOnycew_FMH40SuqOBoateX491/view?usp=sharing)

**Supplementary Video 3** | Confocal microscopy images of pancreas-innervating neurons in CG cleared with iDISCO+ demonstrating 3D distribution of pancreas-projecting neurons and the approach used for segmentation and assessment of neural volume using Imaris with neurons color-coded based on their volumes.